American Mineralogist, Volume 62, pages 534–539, 1977

Estimation of K–O distance and tetrahedral rotation angle of K–micas from far-infrared absorption spectral data

HIROSHI TATEYAMA, SUSUMU SHIMODA AND TOSHIO SUDO

Geological and Mineralogical Institute, Faculty of Science
Tokyo University of Education, Tokyo, Japan

Abstract

Far-infrared absorption spectra of K–micas were measured in the range from 200 to 40 cm^{-1}. The writers propose two equations to calculate the K–O bond length and the tetrahedral rotation angle of K–micas respectively, using the data for lattice parameters and frequencies of vibrations in far-infrared absorption spectra. The equations are as follows:

$$p = 3.676 - 0.0076x$$
$$\alpha = \arctan\left(\sqrt{3} - 6\sqrt{p^2 - 0.25(d_{001} - 6.642)^2}/b\right)$$

where α, p, d_{001}, b, and x are the tetrahedral rotation angle, potassium–oxygen bond length, interplanar spacing, b-lattice parameter, and observed frequency of the K–O stretching vibration in wave numbers respectively.

Introduction

Far-infrared absorption spectra of micas have been observed by a few investigators. Ishii *et al.* (1967, 1969) reported the far-infrared absorption spectra of natural and synthetic micas, and assigned the strong bands occuring in the 120–60 cm^{-1} region to the potassium–oxygen (K–O) stretching vibration because of lack of these bands in pyrophyllite and talc. The relation between the structural data for K–O distance and the frequency of far-infrared absorption band assigned to K–O stretching vibration has not been discussed. We propose an equation to estimate the K–O distance on the basis of the frequency of K–O stretching vibration.

To predict the ditrigonal distortion in micas, many authors [Radoslovich and Norrish (1962), Donnay *et al.* (1964), Franzini (1969), McCauley and Newnham (1971), Hazen and Burnham (1973)] developed equations using lattice parameters, chemical compositions, or both of them. We also propose a new equation to calculate the tetrahedral rotation angle, using lattice parameters and the estimated K–O distance.

Experimental

The samples used in the present experiment are grouped as follows: (A) celadonite and synthetic tetrasilicic Mg and Ni micas, (B) muscovite and fuchsite, (C) clay micas, (D) Li–micas, and (E) phlogopite, biotite, and lepidomelane. Each sample was pulverized to fine powder, which was then held between two polyethylene sheets, and the spectra were determined using a 070 Hitachi Interferometric Spectrometer with the following operating conditions: beam splitter, 12 microns; range, 4; time constant, 0.4. An observational error is estimated to be within $\pm$ 1 cm^{-1}.

Result and discussion

Far-infrared absorption spectra have been determined in the range of frequencies 200–40 cm^{-1}, as shown in Figure 1. The frequencies of the bands assigned to the K–O stretching vibration of the present samples are as shown in Table 1, in which the structural formulas and lattice parameters are also cited. The detailed structural data have not been obtained from the present samples, except Mg^{IV} mica (Tateyama *et al.*, 1974). From the literature, detailed structural data of K–micas were selected and compiled in Table 2. Each of the measured values of the frequencies of the far-infrared absorption bands may be assumed to be common to micas having similar chemical compositions. To illustrate in Table 2, 108 cm^{-1} frequency may be ascribed to samples 1 and 2, 96 cm^{-1} to 3, 95 cm^{-1} to 4 and 5, 90 cm^{-1} to 6, 7, 8, 9,

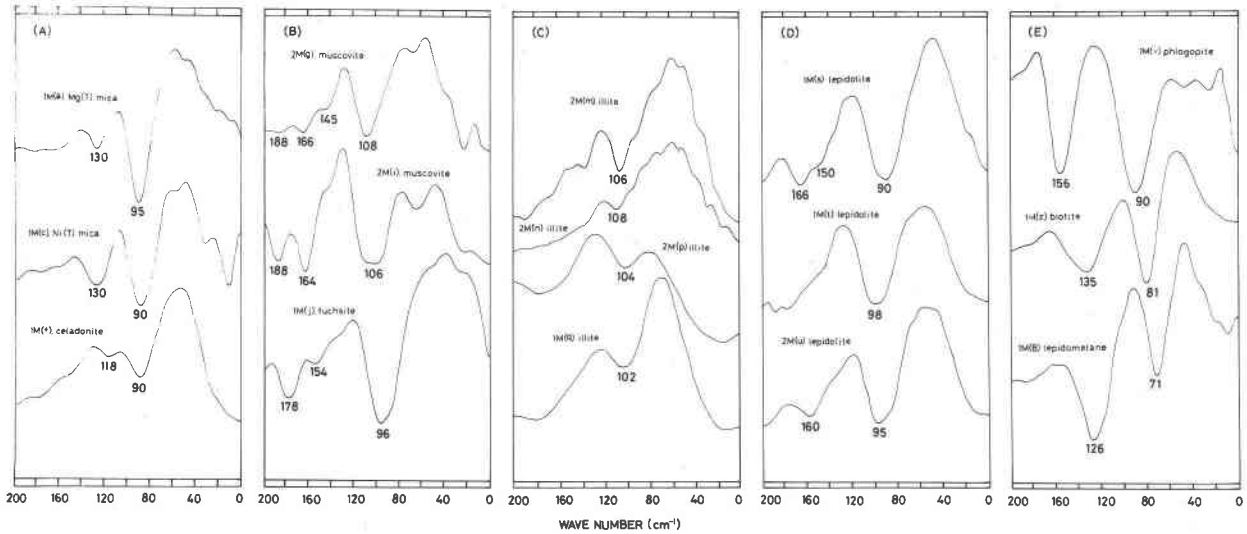

Fig. 1. Far-infrared absorption spectra of some K-micas; (A) tetrasilicic micas, (B): dioctahedral micas, (C): mica clays, (D) Li-micas, (E) trioctahedral micas. The notations correspond to those in Table 4.

Table 1. Far-infrared absorption spectra (frequencies) of some K-micas; structural formulas and lattice parameters are also given

specimens	structural formulas	lattice parameters b_o (Å)	lattice parameters d_o (Å)	F.I.R. (cm^{-1})
2M(1) muscovite	$(K_{0.75}Na_{0.14})(Al_{1.82}Mg_{0.18}Fe_{0.04})(Si_{3.04}Al_{0.96})O_{10}(OH)_2$	8.997	9.948	108
2M(2) fuchsite	$(K_{0.84}Na_{0.05})(Al_{1.25}Mg_{0.51}Cr_{0.14})(Si_{3.54}Al_{0.46})O_{10}(OH)_2$	9.049	9.930	96
2M(3) lepidolite	$(K_{0.92}Na_{0.06})(Al_{1.33}Li_{1.01}Mg_{0.14})(Si_{3.39}Al_{0.71})O_{10}(F_{1.01}OH_{1.02})$	9.030	9.894	95
1M(4) phlogopite	$(K_{0.75}Na_{0.10})(Mg_{2.77}Al_{0.20}Fe_{0.09})(Si_{2.75}Al_{1.25})O_{10}(OH)_2$	9.277	10.066	90
1M(5) lepidolite	$(K_{0.92}Na_{0.04})(Li_{1.72}Al_{1.13}Mn_{0.20})(Si_{3.60}Al_{0.40})O_{10}(F_{1.77}OH_{0.43})$	9.015	9.889	90
1M(6) Mg(IV) mica	$(K_{0.96}Na_{0.04})(Mg_{2.84})(Si_{3.63}Mg_{0.30}Al_{0.30}Fe_{0.04})O_{10}(OH)_2$	9.238	10.129	86
1M(7) lepidomelane	$(K_{0.67}Na_{0.06})(Fe_{2.11}Mg_{0.33}Fe_{0.44})(Si_{2.42}Al_{1.58})O_{10}(OH)_2$	9.308	10.129	71

The localities of the micas used for this study are as follows: 2M(1) muscovite, Ishikawayama, Fukushima Prefecture; 2M(2) fuchsite, Nagatoro, Saitama Prefecture; 2M(3) lepidolite, Nagatare, Fukuoka Prefecture; 1M(4) phlogopite, Korea; 1M(5) lepidolite, Sakihama, Iwate Prefecture; 1M(6) Mg(IV) mica, synthesis; 1M(7) lepidomelane, Iizaka, Fukushima Prefecture. The source of data for structural formulas of the micas: 2M(3), Harada et al (1976); 1M(4), Ishii et al (1967); 1M(5), Harada et al (1976). 1M,2M : polytypes. F.I.R. : far infrared absorption (frequency)

Table 2. Detailed structural data for K-micas previously analysed

specimens	K-O_{inner} distances (Å)	lattice parameters b_o (Å)	lattice parameters d_{001} (Å)	octahedral sheet (O) measured values (Å)	tetrahedral sheet (T) measured values (Å)
1. muscovite	2.855	9.008	9.973	2.148	2.217
2. muscovite	2.857	9.015	9.972	2.132	2.224
3. phengite	2.970	9.038	9.918	2.144	2.218
4. lepdiolite	2.980	9.032	9.938	2.124	2.226
5. lepidolite	2.976	9.04	9.970	2.122	2.219
6. Li-phlogopite	2.995	9.21	9.976	2.174	2.236
7. phlogopite	2.970	9.204	10.009	2.182	2.236
8. phlogopite	2.969	9.190	9.998	2.194	2.335
9. phlogopite	2.965	9.206	10.080	2.188	2.237
10. F-phlogopite	3.006	9.183	9.985	2.200	2.212
11. F-phlogopite	2.987	9.195	9.978	2.172	2.238
12. polilithionite	3.000	8.968	9.863	2.144	2.222
13. Mg(IV) mica	3.061	9.238	10.129	2.250	2.209
14. annite	3.144	9.324	10.093	2.232	2.240
15. Fe-biotite	3.135	9.311	10.010	2.112	2.280
mean value				2.168	2.237

Source of data: 1, Güven (1971); 2, Rothbauer (1971); 3, Güven (1971); 4, Takeda et al (1971); 5, Sartori et al (1973); 6, Takeda and Donnay (1966); 7, Joswig (1972); 8, Hazen and Burnham (1973); 9, Rayner (1974); 10, McCauley et al (1973); 11, Takeda and Morison (1975); 12, Takeda and Buenham (1969); 13, Tateyama et al (1974); 14, Hazen and Burnham (1973); 15 Tepkin et al (1969).

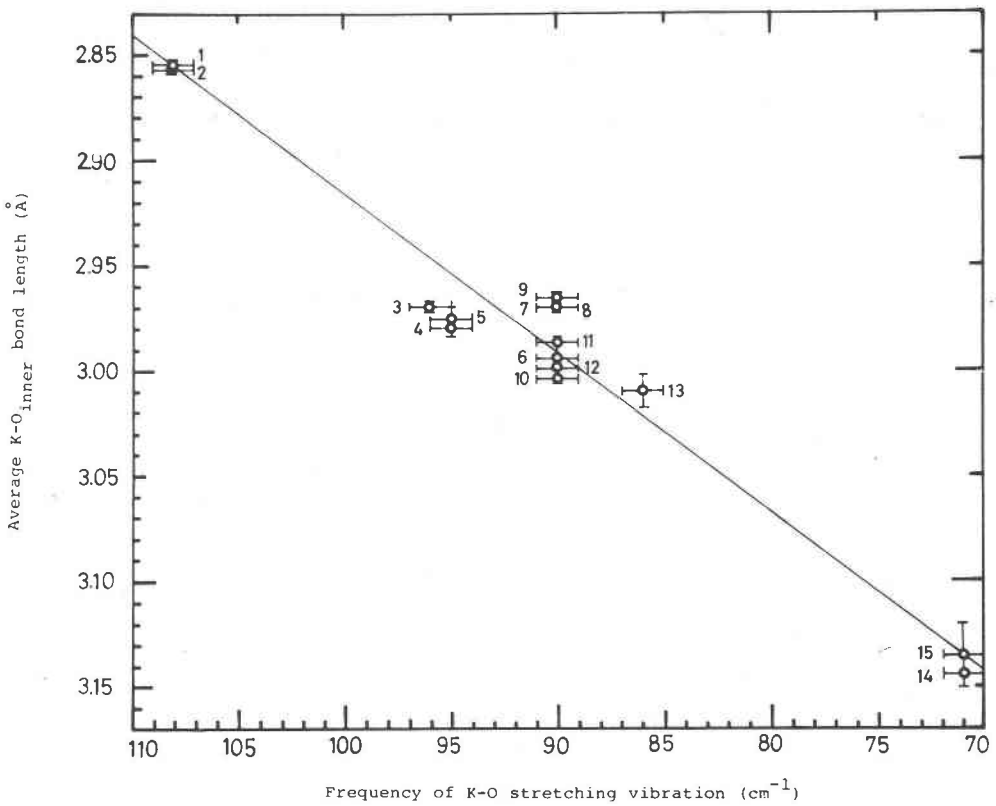

Fig. 2. Relationship between the frequency of the far-infrared absorption band and the $K-O_{inner}$ distance.

10, 11, and 12, 86 cm^{-1} to 13, 71 cm^{-1} to 14 and 15 (Table 2).

In an ideal structural model, the interlayer cation of micas is surrounded by twelve basal oxygens (O_{basal}), among which six are in the layer above and the other six are in the layer below. For most micas now known in some detail, the network of silica tetrahedra—ideally hexagonal—is distorted to a ditrigonal symmetry. Among the twelve oxygens, six oxygens (three above and three below) are located closer to an interlayer cation than the other six oxygens. The K–O bond lengths are divided into two: $K-O_{inner}$ and $K-O_{outer}$ bond lengths.

The far-infrared absorption spectra can be assigned to the K–O stretching vibration. It is expected that the frequencies may vary in a correlative relation with the K–O distance. However, when K–O distances are compared with the frequencies in Table 2, which were measured directly on some samples or ascribed to the other samples, it is noticed that in general the frequencies vary in a clear linear correlative relation with $K-O_{inner}$ distances, rather than with the $K-O_{outer}$ distances or the mean value $K-O_{inner}$ and $K-O_{outer}$ distances. For example, the frequencies do not vary in a simple correlative relation with the mean value of $K-O_{inner}$ and $K-O_{outer}$ distances as illustrated: muscovite (108 cm^{-1}, 3.11 A), lepidolite (95 cm^{-1}, 3.10 A), and polylithionite (90 cm^{-1}, 3.07 A).

Table 3. Tetrahedral rotation angles calculated by the writers' method compared with the values calculated by the methods of the other authors

	α(1)	α(2)	$D\alpha^2$	α(3)	$D\alpha^3$	α(4)	$D\alpha^4$
1.	11°21'	10°37'	44'	12°12'	51'	16°2'	281'
2.	11°22'	10°40'	42'	12°0'	38'	15°18'	236'
3.	6°3'	6°2'	1'	3°47'	136'	13°46'	463'
4.	5°3'	5°54'	51'			13°34'	451'
5.	6°27'	6°23'	4'			13°30'	423'
6.	6°12'	6°28'	16'	4°28'	104'	8°55'	163'
7.	7°40'	6°49'	51'	9°54'	134'	11°35'	295'
8.	7°30'	6°41'	49'	6°13'	77'	11°45'	255'
9.	8°30'	7°44'	46'	7°28'	62'	12°2'	212'
10.	5°3'	6°19'	76'	6°37'	94'	11°45'	402'
11.	6°30'	6°21'	9'	6°37'	7'	11°45'	315'
12.	3°0'	2°36'	24'	2°51'	9'	11°45'	525'
13.	7°6'	7°19'	13'	4°21'	165'	7°49'	43'
14.	1°30'	2°39'	69'	4°30'	180'	8°1'	391'
15.	1°0'	1°32'	32'	5°55'	295'	9°19'	499'
Average Dα			35'		104'		314'

Sample numbers correspond to those in Table 2. α(1): values obtained by the crystal structure analyses. α(2): calculated by the present method. α(3): calculated by the method of McCauley et al (1971). α(4): calculated by the method of Donnay et al (1964). $D\alpha^2$, $D\alpha^3$, $D\alpha^4$: difference between α(1)–α(2), α(1)–α(3), α(1)–α(4) respectively.

Table 4. Far-infrared absorption spectra (frequencies) of additional samples of K-micas, and tetrahedral rotation angles calculated by the writers' method compared with those calculated by the methods of the other authors

		F.I.R. (cm^{-1})	b_o (Å)	d_o (Å)	α(1)	α(2)	α(3)
(I)	Tetrasilicic micas						
1M(a)	Mg(T) mica	95 (s)	9.099	10.040	7°53'	*	6°50'
1M(b)	Mg(T) mica	80 (b)	9.185	10.270	6°36'	*	
1M(c)	Ni(T) mica	90 (s)	9.086	10.009	6°38'	*	7°29'
1M(d)	Ni(T) mica	90 (s)	9.069	9.945	4°39'	*	8°16'
1M(e)	celadonite	90 (b)	9.066	9.998	5°17'	*	8°23'
1M(f)	celadonite	90 (b)	9.060	10.060	6°1'	*	8°38'
(II)	Dioctahedral micas						
2M(g)	muscovite	108 (s)	8.997	9.948	10°10'	10°59'	16°11'
2M(h)	muscovite	96 (s)	9.161	10.087	9°28'		11°45'
2M(i)	muscovite	106 (s)	9.019	9.959	9°50'		
1M(j)	fuchsite	96 (s)	9.030	10.020	7°36'	6°26'	14°8'
1M(k)	fuchsite	94 (s)	9.077	9.970	6°25'	6°39'	12°25'
2M(l)	fuchsite	96 (s)	9.049	9.930	6°19'	2°19'	12°17'
(III)	Mica clays						
2M(m)	illite	106 (s)	9.00	10.009	10°20'	12°30'	16°7'
2M(n)	illite	108 (s)	9.00	9.972	10°31'	12°30'	16°0'
2M(o)	illite	108 (s)	8.993	9.988	10°40'		
2M(p)	illite	104 (s)	8.990	10.009	9°32'		
1M(q)	illite	102 (b)	9.026	10.0	9°3'	12°0'	15°48'
1M(r)	illite	100 (s)	9.007	10.005	8°38'		
(IV)	Li-micas						
1M(s)	lepidolite	90 (s)	9.015	9.889	3°23'	6°1'	13°31'
1M(t)	lepidolite	98 (s)	9.020	9.878	6°3'	6°7'	13°30'
2M(u)	lepidolite	95 (s)	9.030	9.894	5°20'	11°48'	14°12'
(V)	Trioctahedral micas						
1M(v)	phlogopite	90 (s)	9.277	10.066	8°18'	9°8'	11°52'
1M(w)	phlogopite	92 (s)	9.209	10.030	7°49'		
1M(x)	biotite	83 (s)	9.243	10.089	5°50'	9°54'	11°36'
1M(y)	biotite	92 (s)	9.202	10.020	7°37'	12°34'	13°0'
1M(z)	biotite	81 (s)	9.260	10.109	5°35'		
1M(A)	biotite	92 (s)	9.209	10.030	7°48'		
1M(B)	lepidomelane	71 (s)	9.308	10.129	3°56'	8°28'	11°29'
1M(C)	lepidomelane	90 (b)	9.184	10.002	6°32'	19°20'	15°32'

*The localities and references of micas used for this study are as follows: 1M(a) Mg(T) mica, $KMg_{2.5}Si_4O_{10}(OH)_2$ synthesized by Tateyama; 1M(c) Ni(T) mica, $KNi_{2.5}Si_4O_{10}(OH)_2$ synthesized by Tateyama; 1M(e) celadonite, Oya, Tochigi Pref. (Kohyama et al., 1971); 1M(f) celadonite, Taiheizan, Akita Pref. (Kimbara and Shimoda, 1973); 2M(i) muscovite, Madagascar; 1M(j) fuchsite, Setogawa, Shizuoka Pref.; 1M(k) fuchsite, Ouro Ptero, Brazil; 2M(m) illite, Furikusa, Aichi Pref.; 2M(n) illite, Ugusu, Shizuoka Pref.; 2M(o) illite, Goto, Nagasaki Pref. (Tomita and Sudo, 1968); 2M(p) illite, Seshido, Fukushima Pref.; 1M(q) illite, Murakami Niigata Pref.; 1M(r) illite, Kamikita, Aomori Pref.; 1M(t) lepidolite, Suisawa, Mie Pref. (Harada et al, 1976); 1M(w) phlogopite, Madagascar; 1M(x) biotite, Basal B1, Switzerland; 1M(z) biotite, Hase, Ibaragi Pref.. The localities of the micas of 2M(g), 2M(l), 1M(s), 2M(u), 1M(v) and 1M(B) correspond to those of 2M(1), 2M(2), 1M(3), 1M(4), 1M(5) and 1M(7) in Table 1 respectively. The calculated tetrahedral rotation angles (α(2), α(3) and α(4)) correspond to those obtained by the methods listed in Table 2. F.I.R., far infrared absorption (frequency). b, broad; s, sharp. b and d, heated at 700°C for 1 hour; h, heated at 800°C for 1 hour; A and C, heated at 800°C for 14 hours. *: negative α-value.*

By the least-square method, the most probable linear relation (Fig. 2) between the frequency (x) and the K–O_{inner} distance (p) is given by

$$p = 3.676 - 0.0076x. \quad (1)$$

In the mica structure the sum of the thicknesses of two tetrahedral layers, $2T$, an octahedral layer, O,

and an interlayer, y, is equal to the basal interplanar spacing, d_{001}. Thus

$$y = d_{001} - O - 2T. \quad (2)$$

From the structural data for the previously analysed micas, the average thickness of a tetrahedral sheet is 2.237 A (Table 2) and the mean value of the thickness of the octahedral sheet is 2.168 A, thus:

$$y = d_{001} - 6.642. \quad (3)$$

From the ideal ditrigonal model, the K–O_{inner} bond length (p) is given by,

$$p = \{[2H\sin(60° - \alpha)/\sqrt{3}]^2 + 0.25y^2\}^{1/2}, \quad (4)$$

where H and α are the tetrahedral O_{basal}–O_{basal} bond length and the tetrahedral rotation angle respectively. The value of H is obtained from the geometry of an undistorted tetrahedron as:

$$H = 2\sqrt{2}d_t/\sqrt{3}, \quad (5)$$

where d_t is the tetrahedral T–O bond length. Equation (4) is then rewritten as:

$$p = \{[4\sqrt{2}d_t \sin(60° - \alpha)/3]^2 + 0.25y^2\}^{1/2} \quad (6)$$

d_t was given by Donnay *et al.* (1964) as:

$$d_t = b/(4\sqrt{2}\cos\alpha), \quad (7)$$

where b is the b lattice parameter.
Then the tetrahedral rotation angle can be given by:

$$\alpha = \arctan\left(\sqrt{3} - 6\sqrt{p^2 - y^2/b}\right). \quad (8)$$

Then equation (7) may be written as:

$$\alpha = \arctan\left(\sqrt{3} - 6\sqrt{p^2 - 0.25(d_{001} - 6.642)^2/b}\right) \quad (9)$$

Using equations (8) and (9), the tetrahedral rotation angle can be estimated from p and y; p can be estimated by the frequency of the far-infrared absorption spectrum, and y can be found from d_{001} and b, both of which are obtained from the X-ray powder diffraction data.

The tetrahedral rotation angles calculated by the present method are compared with the values calculated by the earlier methods of McCauley *et al.* (1973), and Donnay *et al.* (1964), and also with the values obtained by the structural analysis as shown in Table 3. The present values are in better agreement with the values obtained by the structural analyses than those obtained by the earlier methods. The tetrahedral rotation angles of some additional samples of K–micas calculated by the present method using the frequencies of the far-infrared absorption spectra, b and d_{001} values are compared with the values calculated by the earlier methods as shown in Table 4.

The writers consider that the use of the far-infrared data coupled with cell-dimension data obtained from X-ray powder diffraction patterns will allow estimation of the tetrahedral rotation angle of K–micas.

Acknowledgments

We thank Drs. K. Kimbara of Geological Survey of Japan, N. Kohyama of National Institute of Industrial Health, M. Inomata, and K. Takasawa for providing the samples. A part of the expense of the study was defrayed by a grant-in-aid for science research from the Ministry of Education.

References

Donnay, G., J. D. H. Donnay and H. Takeda (1964) Trioctahedral one-layer micas. II. Prediction of the structure from composition and cell dimensions. *Acta Crystallogr., 17,* 1374–1381.

Drits, V. A. (1969) Some general remarks on the structure of trioctahedral micas. *Proc. Int. Clay Conf., 1,* 51–59.

Franzini, M. (1969) The *A* and *B* mica layers and the crystal structure of sheet silicates. *Contrib. Mineral. Petrol., 21,* 203–224.

Güven, N. (1971) The crystal structures of $2M_1$ phengite and $2M_1$ muscovite. *Z. Kristallogr., 134,* 196–212.

Harada, K., M. Honda, K. Nagashima and S. Kanisawa (1976) Masutomilite, manganese analogue of zinnwaldite, with special reference to masutomilite–lepidolite–zinnwaldite series. *Mineral. J., 8,* 95–109.

Hazen, R. M. and C. W. Burnham (1973) The crystal structures of one-layer phlogopite and annite. *Am. Mineral., 58,* 889–900.

Ishii, M., M. Nakahira and H. Takeda (1969) Far infrared absorption spectra of micas. *Proc. Int. Clay Conf., 1,* 247–259.

———, T. Shimanouchi and M. Nakahira (1967) Far infrared absorption spectra of layer silicates. *Inorg. Chim. Acta, 1,* 387–392.

Kimbara, K. and S. Shimoda (1973) A ferric celadonite in amygdals of dolerite at Taiheizan, Akita Pref., Japan. *Clay Sci., 4,* 143–150.

Kohyama, N., S. Shimoda and T. Sudo (1971) Celadonite in the tuff of Oya, Tochigi Prefecture, Japan. *Mineral. J., 6,* 299–312.

McCauley, J. M. and R. E. Newnham (1971) Origin and prediction of ditrigonal distortions in micas. *Am. Mineral., 56,* 1626–1638.

———, ——— and G. V. Gibbs (1973) Crystal structure analysis of synthetic fluorphlogopite. *Am. Mineral., 58,* 249–254.

Radoslovich, E. W. and K. Norrish (1962) The cell dimensions and symmetry of layer lattice silicates. I. Some structural considerations. *Am. Mineral., 47,* 599–616.

Rayner, J. H. (1974) The crystal structure of phlogopite by neutron diffraction. *Mineral. Mag., 39,* 850–856.

Rothbauer, R. (1971) Untersuchung eines $2M_1$-Muscovite mit Neutronenstrahlen. *Neues Jahrb. Mineral. Monatsh.,* 143–154.

Sartori, F., M. Franzini and S. Merlino (1973) Crystal structure of a $2M_2$ lepidolite. *Acta Crystallogr., B 29,* 573–578.

Takeda, H. and C. W. Burnham (1969) Fluorpolylithionite: A lithium mica with nearly hexagonal $Si_2O_5^2$ ring. *Mineral. J., 6,* 102–109.

——— and J. D. H. Donnay (1966) Trioctahedral one-layer micas.

III. Crystal structure of a synthetic lithium fluormica. *Acta Crystallogr., 20,* 638–646.

———, H. Haga and R. Sadanaga (1971) Structural investigation of polymorphic transition between $2M_2$–, $1M$–lepidolite and $2M_1$ muscovite. *Mineral J., 6,* 203–215.

——— and B. Morosin (1975) Comparison of observed and predicted structural parameters of mica at high temperature. *Acta Crystallogr., B31,* 2444–2452.

Tateyama, H., S. Shimoda and T. Sudo (1974) The crystal structure of synthetic Mg^{IV} mica. *Z. Kristallogr., 139,* 196–206.

Tepkin, E. V., V. A. Drits and V. A. Alexandrova (1969) Crystal structure of iron biotite and construction of structural models for trioctahedral micas. *Proc. Int. Clay Conf.,* 43–49.

Tomita, K. and T. Sudo (1968) Interstratified structure formed from pre-heated mica by acid treatment. *Nature, 217,* 1043–1044.

Manuscript received, February 10, 1976; accepted for publication, December 22, 1976.